

## Osmium Metal Studied under High Pressure and Nonhydrostatic Stress

Michelle B. Weinberger,<sup>1,†</sup> Sarah H. Tolbert,<sup>1,\*</sup> and Abby Kavner<sup>2,\*</sup>

<sup>1</sup>Department of Chemistry and Biochemistry, UCLA, Los Angeles, California 90095-1569, USA

<sup>2</sup>Department of Earth and Space Sciences and Institute of Geophysics and Planetary Physics, UCLA, Los Angeles, California 90095-1567, USA

(Received 3 July 2007; published 31 January 2008)

Interest in osmium as an ultra-incompressible material and as an analog for the behavior of iron at high pressure has inspired recent studies of its mechanical properties. We have measured elastic and plastic deformation of Os metal at high pressures using *in situ* high pressure x-ray diffraction in the radial geometry. We show that Os has the highest yield strength observed for any pure metal, supporting up to 10 GPa at a pressure of 26 GPa. Furthermore, our data indicate changes in the nonhydrostatic apparent  $c/a$  ratio and clear lattice preferred orientation effects at pressures above 15 GPa.

DOI: 10.1103/PhysRevLett.100.045506

PACS numbers: 62.20.F-, 61.05.cp, 64.30.-t, 91.60.Gf

Recent attempts to correlate material hardness with other mechanical properties, particularly bulk modulus, have resulted in significant interest in osmium metal. Diamond anvil cell experiments conducted using differing pressure media resulted in measured bulk moduli for osmium that varied between 395 and 462 GPa [1–3], a value rivaling that of diamond (443 GPa) [4]. While the hardness of osmium is low (only 4 GPa [5]), the modulus results have inspired interest in using osmium as a host matrix for the incorporation of small covalent atoms to make superhard materials [6]. Moreover, we show here that even though the hardness of osmium does not compare to its extreme bulk modulus value, it does have a remarkable ability to support differential stress.

Our interest in osmium also stems from the potential analogy between the behavior of iron at high pressures and that of osmium at moderate pressures. Osmium has a hexagonally close-packed crystal structure, similar to that of iron at the conditions of the Earth's core [7]. Predicted trends suggest that, within the transition metals, higher  $Z$  elements in the same periodic group mimic behavior of lower  $Z$  elements, as long as the crystal structures are the same [8]. Success in drawing this correlation between the mechanical properties of osmium and iron could be very useful in the ongoing quest to characterize the behavior of the Earth's core. Seismic anomalies show that the sound velocities through the core in the north-south direction are significantly faster than in the east-west [9].

To elucidate the unique mechanical properties of Os, we performed nonhydrostatic *in situ* high pressure diffraction experiments to determine its strength and deformation behavior using beam line X17C at the NSLS [11–13]. Osmium powder was loaded into a preindented Be gasket hole 100  $\mu\text{m}$  in diameter and  $\sim 30$   $\mu\text{m}$  thick. The sample was compressed in a diamond anvil cell equipped with 300  $\mu\text{m}$  diamond culets without inclusion of a pressure medium to intentionally create nonhydrostatic pressure conditions. In this experiment, a  $10 \times 10$   $\mu\text{m}$  x-ray beam was directed through the beryllium gasket, between the diamond faces, and into the sample, rather than through the

diamonds, as in traditional diamond anvil cell experiments [12,14,15]. Energy dispersive diffraction patterns were collected at room temperature and pressure, and at six elevated pressures. At each pressure, eight diffraction patterns were collected as the diamond anvil cell was rotated through angle  $\psi$  about the x-ray beam. The angle between the x-ray beam and the detector,  $2\theta$ , was calibrated with a gold foil and remained fixed at  $10.002 \pm 0.002^\circ$ .

In the nonhydrostatic diamond anvil cell sample chamber, the general stress state is assumed to be cylindrically symmetric, with the maximum principal stress in the diamond anvil normal direction, and the minimum principal stress in the radial (gasketed) direction. As the cell is rotated about  $\psi$  from the minimum to the maximum stress directions, the diffraction peaks shift to higher energy, corresponding to lower  $d$  spacing (Fig. 1). As the compression on the sample is increased, the difference between  $d_{\text{max}}$ , (the  $d$  spacing corresponding to the maximum stress direction,  $\psi = 0^\circ$ ) and  $d_{\text{min}}$ , (the  $d$  spacing measured in the minimum stress direction,  $\psi = 90^\circ$ ) increases indicating a larger supported differential stress. The hydrostatic value is calculated from a geometric average of the  $d$  spacings, and is equal to  $(2d_{\text{min}} + d_{\text{max}})/3$  (Fig. 1).

The relationship between the measured  $d$  spacing ( $d_m(hkl)$ ) and the angle  $\psi$  is given by  $d_m(hkl) = d_p(hkl) \times [1 + (1-3\cos^2\psi)Q(hkl)]$ , where  $d_p(hkl)$  is the hydrostatic  $d$  spacing and  $Q(hkl) = t/3\{\alpha[2G_R(hkl)]^{-1} + (1-\alpha) \times (2G_V)^{-1}\}$ . Here  $t$  is the differential stress supported by the sample,  $G_R$  and  $G_V$  are the shear moduli under Reuss (constant stress) and Voigt (constant strain) bounds, respectively, and  $\alpha$  is between 0 and 1 [15]. For an elastically isotropic material,  $G_R$  is equal to  $G_V$ .

One threshold for plastic deformation is the von Mises yield criterion [16], given by  $t = \sigma_1 - \sigma_3 \leq 2\tau = \sigma_y$ , where  $\tau$  is the shear strength and  $\sigma_y$  is the yield strength. Therefore, a measurement of the elastically supported differential stress,  $t$ , provides a lower-bound estimate on the material's yield strength,  $\sigma_y$ . As the diamond cell compression increases, the stiffness of the individual

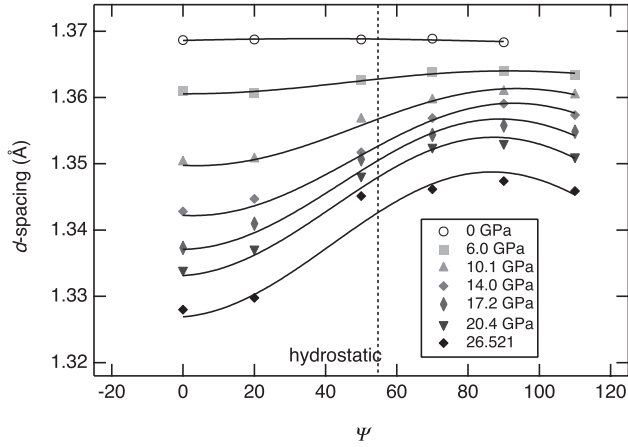


FIG. 1.  $d$  spacing of the (110) diffraction peak as a function of  $\psi$  and pressure. The data are shown as symbols; smooth curves show the  $1-3\cos^2\psi$  fits through each data set. The intersection of the dotted line with the curves shows the hydrostatic value of the  $d$  spacing at each pressure step.

planes controls their response to the difference between the stresses in the diamond normal and radial directions. In an anisotropic crystal, such as the hexagonal crystal structure of osmium, structural lattice anisotropy affects the differential stress that can be supported.

The elastic anisotropy [17] is incorporated in the strain theory used for the analysis of this data [11] via the lattice-dependent Reuss bound on the shear modulus, given by  $[G_R(hkl)]^{-1} = (2S_{11} - S_{12} - S_{13}) + (-5S_{11} + S_{12} + 5S_{13} - S_{33} + 3S_{44})B + (3S_{11} - 6S_{13} + 3S_{33} - 3S_{44})B^2$  where  $B = 3a^2l^2/[4c^2(h^2 + hk + k^2) + 3a^2l^2]$ ,  $h$ ,  $k$ , and  $l$  are Miller indices,  $a$  and  $c$  are the unit cell parameters, and  $[S_{ij}]$  are the elastic compliances, obtained by inverting the elastic stiffness constants,  $[C_{ij}]_s$ . The Voigt bound on the shear modulus is independent of  $hkl$ , and is given by

$$G_V = \frac{2C_{11} + C_{33}}{15} + \frac{2C_{13} + C_{12}}{15} + \frac{2C_{44} + \frac{1}{2}(C_{11} - C_{12})}{5}$$

To date, these constants have not been experimentally measured for Os; therefore we considered two sets of theoretically generated  $[C_{ij}]_s$  [18,19]. One set [18] implied a bulk modulus value 20% greater than the measured value of 395 GPa [3]. Therefore we use values provided by Ref. [19]. Shear moduli at both bounds were calculated from the five independent elastic constants for Os, and then extrapolated to high pressure using  $dG/dP = 1.5$ . Experiments show that this is a good average of the  $dG/dP$  values of many types of silicates, oxides, and metals [20]. The calculated  $G_V$  at 26.5 GPa is 319 GPa. At the same pressure, values for  $G_R$  for the lattice planes range from 312 GPa for the (101) plane to 348 GPa for the (002) plane.

Radial diffraction data were obtained at six elevated pressures, from 6 GPa to 26.5 GPa, and six well-resolved diffraction peaks were used in the study: (100), (002), (101), (102), (110), and (103). The pressures in this ex-

periment were determined by comparing the previously measured  $P(V)$  equation of state data to the volumes measured in this experiment [3]. The differential stress calculated using the Voigt bound on the shear modulus provides a strongly lattice-dependent differential stress (Fig. 2). At 25 GPa Os supports a differential stress up to 10.0 GPa [for the (110) plane]. This  $t$  value is over twice that measured for rhenium, previously thought to be the strongest of elemental metals ( $t \sim 4.75$  GPa at  $P \sim 25$  GPa) [12].

If the measured  $t$  values are considered a lower bound on the shear strength, this suggests that osmium plastically deforms less easily than any other pure metal. Similar data in both magnitude and lattice dependence are also observed when the  $(hkl)$ -dependent Reuss bounds on the shear moduli are used. This has two possible implications: either the observed anisotropy arises from a lattice-dependent yield strength (i.e., a plastic anisotropy rather than an elastic anisotropy), or the calculated elastic constants are incorrect. The plateau in the differential stress supported by the (002) plane suggests that it has reached its actual yield strength at the pressures achieved in this experiment. In contrast, the differential stress the other planes are able to support appears to be steadily increasing with increasing pressure. The plateau in only the (002) plane lends support to the hypothesis of a lattice-dependent yield strength.

The high strength measured for osmium has significant implications for the experimental determination of its equation of state. Although the inclusion of pressure medium is intended to create hydrostatic conditions in the sample, all known pressure media freeze by 15 GPa [21]. Consequently, the sample is likely subjected to some non-hydrostatic stress. In conventional diamond anvil cell experiments, the diffraction is collected in the diamond normal direction. Therefore any deviation from hydrosta-

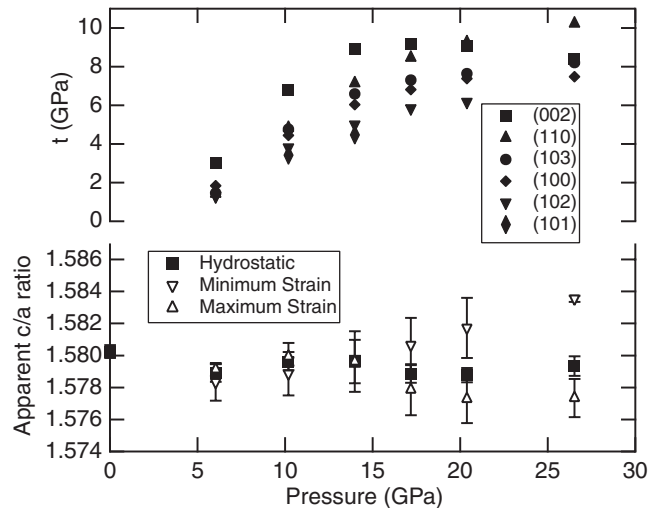


FIG. 2. Pressure dependence of differential stress (top) and apparent  $c/a$  ratio in maximum, minimum, and hydrostatic stress directions (bottom).

ticity results in a measurement that preferentially samples lattice planes oriented such that they experience the minimum stress, providing an underestimate of volumetric strain. Our measurements allow us to calculate potential errors in equation of state measurements as a function of degree of nonhydrostaticity. For example, if the pressure medium can support a differential stress of 2.7 GPa at 55 GPa (e.g., argon) [22], a material with a bulk modulus of 396 GPa would appear to have a bulk modulus of 450 GPa when  $B_0'$  is fixed to 4. This higher value is in excellent agreement with the measurements made by Cynn *et al.* on Os in an Ar medium [1].

Because of the hexagonal crystal structure of osmium, an examination of the  $c/a$  ratio can be used to provide additional information on nonhydrostatic deformation at high pressure. The geometry of the radial diffraction technique allows us to measure apparent  $c/a$  ratios in the maximum, minimum, and hydrostatic stress directions (Fig. 2). At ambient pressure, the  $c/a$  ratio is equal to  $1.5802 \pm 0.0008$ . There is a small drop down to  $1.5789 \pm 0.0011$  at 5 GPa and the value is then approximately constant across the pressure range studied. Up to 15 GPa, the  $c/a$  ratios in the minimum and maximum stress direction agree very well with the hydrostatic value; however, at higher pressures, the apparent  $c/a$  ratio in the minimum and maximum stress directions diverge—increasing in the minimum strain direction (up to  $1.5835 \pm 0.0004$  at 26 GPa), and decreasing in the maximum stress direction (falling to  $1.5773 \pm 0.0024$  at the highest pressure). The increasing apparent  $c/a$  ratio observed in the minimum stress direction is consistent with the  $c/a$  ratios measured in the diamond normal direction in conventional diamond cell experiments [3]. This suggests that, above the pressure where all known pressure media freeze (15 GPa), the experiments are in fact nonhydrostatic. In the diamond anvil cell geometry where diffraction is collected through the diamonds, the planes that satisfy the Bragg equation for diffraction are ones that are perpendicular to the diamond faces and are subjected to stress in the radial (minimum stress) direction. As a result, data collected from experiments that are intended to be hydrostatic are in fact measuring diffraction from the minimum stress direction, resulting in increased apparent  $c/a$  ratios.

A closer examination of our  $c/a$  data indicates that the drop between room pressure and 6 GPa, and the discontinuity we observe at  $\sim 15$  GPa are also apparent in all published Os high pressure data [1–3]; however, these discontinuities were assumed to arise from experimental scatter. Since we observe similar patterns we note their consistency and suggest that this behavior relates to an intrinsic property of Os. One possibility is that the  $c/a$  ratio is recording an equilibrium property such as a pressure-induced change in electronic structure. If this is the case, then potentially interesting implications for Earth's core exist, to the extent that Os in this pressure range may be considered an analogue for the behavior of

Fe at high pressures and high temperatures. A second possibility is that the evolving apparent  $c/a$  ratio arises from a mechanically induced change in rheological properties, such as a change in the dominant slip system from prismatic to basal slip, which appears to occur at  $\sim 15$  GPa (see below).

Finally, these experiments provide unique information about lattice preferred orientations generated at high strain. The data show distinct evidence of development of lattice preferred orientation as pressure is increased (Fig. 3). At  $\psi = 90^\circ$  (minimum stress direction), the intensity of the (101) peak increases, while the intensity of the (002) peak decreases. This trend is reversed at  $\psi = 0^\circ$  (maximum stress direction) where the (002) intensity increases while (101) decreases. These changes in intensity as the sample pressure increases indicate that the sample is preferentially aligning the least strong [001] direction with the primary stress direction. This observation of preferential alignment of hcp Os is in agreement with experimental data on cobalt, as well as theoretically modeled behavior of hcp materials [23]. Through modeling experiments, the prismatic and basal slip systems have been shown to dominate the plastic deformation mechanism of hexagonally close-packed materials. In materials with low  $c/a$  ratios, such as  $\epsilon$ -Fe at high pressure, as well as Zr and Ti, the prismatic slip system dominates at low strain. As the strain increases, the basal slip system becomes the dominant mechanism, expediting the alignment of the [001] direction. The plateau in the ability of the (002) plane to support differential stress at  $\sim 15$  GPa corresponds to the pressure where the basal slip system becomes dominant. Other deformation-related behavior that cannot be accounted for by the elasticity analysis is found in the high pressure behavior of the (101) and (102) diffraction lines, which can no longer be fit by the  $1-3\cos^2\psi$  dependence above pressures of 14.0 and 17.2 GPa, respectively.

The elasticity behavior of hexagonal materials has been notoriously difficult to determine using radial diffraction methods. For example, in their analysis of the lattice-

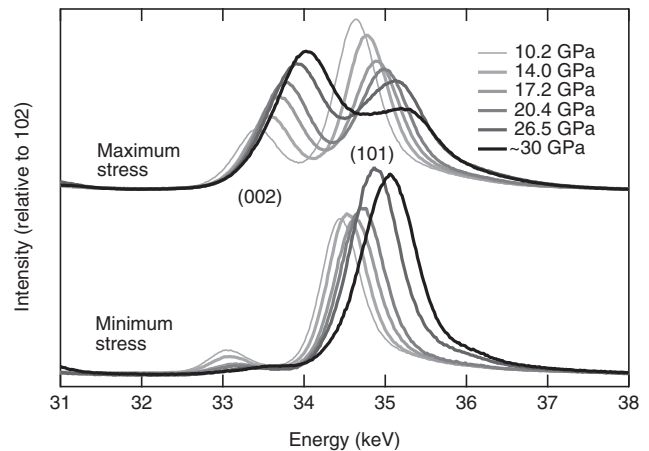


FIG. 3. Evolution of the relative intensities for the Os (002) and (101) diffraction peaks.



dependent strain of rhenium, Duffy *et al.* [12] do not reproduce independently determined elastic constants. This is also observed in conflicting experimental and theoretical information on the elastic anisotropy of Fe at deep Earth pressure conditions [10,24]. It has been suggested that one of the reasons for these discrepancies is the inability to differentiate between elastic lattice anisotropy and lattice-plane dependent strength [25]. Our results on Os highlight this difficulty. We observe distinct changes in lattice-dependent strength and preferred orientation as a function of pressure. At the extreme, the 101 and the 102  $d$  spacings can no longer be fit with the  $\cos^2\psi$  analysis. In addition, we observe that the differential stress of the (110) lattice plane increases continuously with pressure, reaching a value over 10 GPa at the highest pressures achieved in this experiment. At the same time, the orthogonal basal plane, (002), reaches a maximum differential stress value at just 17 GPa, and then decreases with further increase in pressure. We interpret this as a strongly lattice-dependent strength response. However, if we were to interpret these observations as arising solely from elastic lattice behavior, we would be forced to acknowledge a transition in the sense of elastic anisotropy between 15 and 20 GPa. This potential change is reminiscent of radial changes in the anisotropic behavior of Fe in the solid inner core of the Earth [26].

This work was funded by the National Science Foundation under Grants No. EAR-0510914 (A. K.), and No. CMS-0307322 (S. H. T.). Use of the NSLS was supported by the U.S. DOE Office of Basic Energy Science, under Contract No. DE-AC02-98CH10886. We wish to thank J. Hu for assistance in the collection of this data and B. Howard for assistance with the data analysis.

\*Corresponding authors.

akavner@ucla.edu

tolbert@chem.ucla.edu

†Present address: Geophysical Laboratory Carnegie Institution of Washington, 5251 Broad Branch Rd NW, Washington, DC 20015, USA.

- [1] H. Cynn, J. E. Klepeis, and C. S. Yoo, *et al.*, Phys. Rev. Lett. **88**, 135701 (2002).
- [2] F. Occelli, D. L. Farber, and J. Badro *et al.*, Phys. Rev. Lett. **93**, 109901 (2004).
- [3] T. Kenichi, Phys. Rev. B **70**, 012101 (2004).
- [4] I. V. Aleksandrov, A. F. Goncharov, and A. N. Zisman *et al.*, Zh. Eksp. Teor. Fiz. **93**, 680 (1987).
- [5] J. F. Shackelford and W. Alexander, in *CRC Materials Science and Engineering Handbook* (CRC Press, Boca Raton, 2001), 3rd ed.
- [6] R. W. Cumberland, M. B. Weinberger, and J. J. Gilman *et al.*, J. Am. Chem. Soc. **127**, 7264 (2005); H. Y. Chung, M. B. Weinberger, and J. B. Levine *et al.*, Science **316**, 436 (2007).
- [7] R. J. Hemley and H. K. Mao, Int. Geol. Rev. **43**, 1 (2001); Y. Z. Ma, M. Somayazulu, and G. Y. Shen *et al.*, Phys. Earth Planet. Inter. **143–44**, 455 (2004).
- [8] J. H. Rose, R. R. Smith, and F. Guinea *et al.*, Phys. Rev. B **29**, 2963 (1984).
- [9] A. Morelli, A. M. Dziewonski, and J. H. Woodhouse, Geophys. Res. Lett. **13**, 1545 (1986); J. H. Woodhouse, D. Giardini, and X. D. Li, Geophys. Res. Lett. **13**, 1549 (1986); P. M. Shearer, K. M. Toy, and J. A. Orcutt, Nature (London) **333**, 228 (1988); W. J. Su and A. M. Dziewonski, J. Geophys. Res. **100**, 9831 (1995); X. D. Song, Rev. Geophys. **35**, 297 (1997).
- [10] L. Stixrude and R. E. Cohen, Science **267**, 1972 (1995); G. Steinle-Neumann, L. Stixrude, and R. E. Cohen, Phys. Rev. B **60**, 791 (1999).
- [11] A. K. Singh, C. Balasingh, and H. K. Mao *et al.*, J. Appl. Phys. **83**, 7567 (1998). Note. There is an error in one of the equations in this paper, and  $B$  should be equal to  $3a^2l^2/(4c^2(h^2 + hk + k^2) + 3a^2l^2)$ .
- [12] T. S. Duffy, G. Y. Shen, and D. L. Heinz *et al.*, Phys. Rev. B **60**, 15063 (1999).
- [13] T. S. Duffy, R. J. Hemley, and H. K. Mao, Phys. Rev. Lett. **74**, 1371 (1995).
- [14] G. L. Kinsland and W. A. Bassett, Rev. Sci. Instrum. **47**, 130 (1976); R. J. Hemley, H. K. Mao, and G. Y. Shen *et al.*, Science **276**, 1242 (1997).
- [15] A. K. Singh, J. Appl. Phys. **73**, 4278 (1993).
- [16] A. L. Ruoff, Scr. Metall. Mater. **8**, 1161 (1974); A. L. Ruoff, J. Appl. Phys. **46**, 1389 (1975).
- [17] R. F. S. Hearmon, Rev. Mod. Phys. **18**, 409 (1946); R. F. S. Hearmon, Adv. Phys. **5**, 323 (1956).
- [18] L. Fast, J. M. Wills, and B. Johansson *et al.*, Phys. Rev. B **51**, 17431 (1995).
- [19] Y. M. Ma, M. Zhang, and G. Zou (private communication) ( $C_{11} = 777.7$ ;  $C_{12} = 224$ ;  $C_{13} = 223.6$ ;  $C_{33} = 855$ ;  $C_{55} = 269.5$ ;  $C_{66} = 276.85$ ; all GPa).
- [20] D. G. Isaak, in *Handbook of Elastic Properties of Solids, Liquids, and Gases*, edited by M. Levy, H. Bass, R. Stern, and V. Keepens (Academic Press, San Diego, 2001). To examine the error in calculating  $t$  introduced by our assumption of  $dG/dP = 1.5$ , we compare a calculated  $t$  value with one calculated assuming  $dG/dP = 1.0$ . At 26.5 GPa, this difference produces a 4% error in the values of  $t$  calculated. Therefore, we conclude that the  $t$  measurements are robust with respect to assumptions about pressure extrapolation of the elastic constants.
- [21] R. J. Angel, M. Bujak, and J. Zhao *et al.*, J. Appl. Crystallogr. **40**, 26 (2007).
- [22] H. K. Mao, J. Badro, and J. F. Shu *et al.*, J. Phys. Condens. Matter **18**, S963 (2006).
- [23] S. Merkel, N. Miyajima, and D. Antonangeli *et al.*, J. Appl. Phys. **100**, 023510 (2006).
- [24] R. E. Cohen, L. Stixrude, and E. Wasserman, Phys. Rev. B **56**, 8575 (1997); H. K. Mao, J. F. Shu, and G. Y. Shen *et al.*, Nature (London) **396**, 741 (1998); S. Merkel, H. R. Wenk, and P. Gillet *et al.*, Phys. Earth Planet. Inter. **145**, 239 (2004); S. Merkel, J. F. Shu, and P. Gillet *et al.*, J. Geophys. Res. **110** (2005); D. Antonangeli, F. Occelli, and H. Requardt *et al.*, Earth Planet. Sci. Lett. **225**, 243 (2004); D. Antonangeli, S. Merkel, and D. L. Farber, Geophys. Res. Lett. **33**, L24303 (2006).
- [25] D. J. Weidner, L. Li, and M. Davis *et al.*, Geophys. Res. Lett. **31**, L06621 (2004).
- [26] M. Ishii and A. M. Dziewonski, Proc. Natl. Acad. Sci. U.S.A. **99**, 14026 (2002).